Materials Transactions, Vol. 56, No. 6 (2015) pp. 835 to 839

Chemometric Approach for Mechanical Properties Prediction during the Electromagnetic Casting Process

Aleksandra Patarić[1,*], Zvonko Gulišija[1], Branka Jordović[2], Lato Pezo[3], Marija Mihailović[1] and Milentije Stefanović[4]

[1]*Institute for Technology of Nuclear and Other Mineral Raw Materials, Franchet d'Esperey 86, 11000 Belgrade, Serbia*
[2]*Faculty of Technical Sciences, University of Kragujevac, Svetog Save 65, 32000 Čačak, Serbia*
[3]*Institute of General and Physical Chemistry, University of Belgrade, Studentski Trg 12-16, 11000 Belgrade, Serbia*
[4]*Faculty of Engineering, University of Kragujevac, Sestre Janjić 6, 34000 Kragujevac, Serbia*

In this study the mechanical properties (reduction of area, S_0, tensile strength, R_m, yield strength, R_p, and elongation, A) of EN AW 7075 aluminum alloy obtained by electromagnetic casting were investigated at different operating parameters: frequency (V), field strength (T) and current intensity (I). The predictive mathematical models using Response Surface Methodology, with second order polynomial (SOP) regression models, and Artificial Neural Network model (ANN), were afterwards compared to obtained experimental results. Analysis of variance and post-hoc Tukey's HSD test at 95% confidence limit ("honestly significant differences") have been utilised to show significant differences between various samples. SOP models showed good prediction capabilities, with high coefficients of determination (r^2), 0.531–0.977, while ANN model performed even better prediction accuracy: 0.800–0.992. The optimal samples were chosen depending on mechanical properties of the product ($S_0 = 50.49\,mm^2$, $R_m = 405.75\,N\,mm^{-2}$, $R_p = 302.49\,N\,mm^{-2}$, $A = 6.86\%$), using optimal operating parameters ($V = 30\,Hz$, $I = 250\,A$, $T = 18 \times 10^{-3}\,At$). [doi:10.2320/matertrans.M2015058]

(Received February 16, 2015; Accepted March 24, 2015; Published May 25, 2015)

Keywords: *casting, mechanical properties, neural network modeling, prediction, aluminum alloy*

1. Introduction

Electromagnetic casting (EMC) is the technological process developed by introducing the magneto hydrodynamics into the casting process, providing the opportunity which has never been achieved by conventional casting process. Electromagnetic forces, arising from the interaction of Eddy currents induced in the metal by inductor magnetic field, stimulate an increased flow of the fluid, forced convection, more uniform temperature field and weak gravitation influence thus changing the solidification conditions. The conventional casting process contributes to numerous defects which can not be eliminated even with heat treatment as subsequent process.[1,2] There are also some attempts to obtain finer and more homogenous microstructure by addition of some grain refining elements but it revealed as too complicated and not so efficient.[3,4] The advantage of EMC reflects in obtaining a better quality of ingots compared to conventional continuous casting process.[5–8] The obtained structure is finer and more uniform over the cross section, segregation of alloying elements and porosity are reduced, and hence - the mechanical properties are better. Besides, due to the reduced contact pressure which is the result of electromagnetic field effect, between the mold and the metal, the quality of ingot surface is better and there is no need for additional machine processing. It is very important to get better quality of as cast ingots as this process becomes more efficient. There are some published investigations related to the microstructure and mechanical characterization but very little attention was given to the final results prediction from some already achieved experimental data.[9–13] This modeling is aimed to establish the possibility of obtaining the better quality of ingots and shortening the production process through the proper combination of the main operating parameters, frequency (V), field strength (T) and current intensity (I).

The specific objective in this study was to investigate the effect of V, I and T on mechanical properties: reduction of area, S_0, tensile strength, R_m, yield strength, R_p, and elongation, A, and the focus was to determine the optimal mechanical properties, depending on investigated input variables. In the case of EMC of aluminum alloy manufacturing, nonlinear models are founded to be more suitable due to complexity of casting process. Second order polynomial (SOP), using Response Surface Methodology (RSM) and Artificial Neural Network (ANN) models are recognized as a good modeling tools since they provide the solution to the problems from a set of experimental data, and are capable of handling complex systems with nonlinearities and interactions between decision variables.[14] Developed empirical models give a reasonable fit to experimental data and successfully predict mechanical properties and can be used for control of casting processes.

Optimization algorithm used in this study is concerned with finding the maxima of objective functions, subject to constraints.

2. Materials and Methods

The alloy used for experimental casting is EN AW 7075, heat treatable very high strength alloy with wide application in aero and military industry. Despite this, it is characterized by numerous defects occurring during the solidification process, such as: porosity, hot cracks, non-uniform grain size and crystal segregation.

The experimental equipment consists of medium frequency induction furnace with capacity of 100 kg. There is a drainpipe, at the bottom of the furnace, with graphite

*Corresponding author, E-mail: a.pataric@itmns.ac.rs

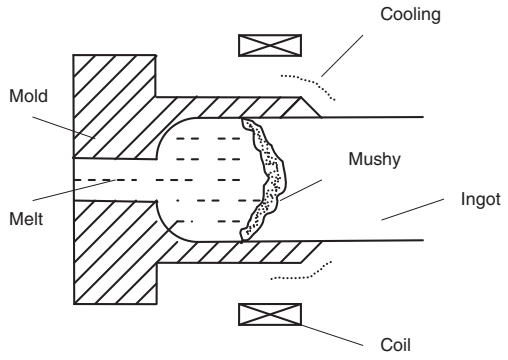

Fig. 1 Schematic illustration of the electromagnetic process.

crystallizer that is intensively cooled with water. The low frequency magnetic field is placed around the crystallizer itself. The schematic illustration of the electromagnetic process is shown at the Fig. 1. The testing samples were taken out of ingots center with a diameter of 90 mm, obtained by vertical continual casting. The casting temperature was in the range of 710–720°C and the average casting speed was 1.5 mm/s. The main operating parameters: V, T and I are combined to obtain and predict the best conditions of EMC. The operating parameters, during the casting of ingots, were strictly controlled and for each frequency of 10 Hz, 30 Hz and 50 Hz, the different current value of 200 A, 250 A and 300 A, and strength of electromagnetic field value of 12000 A_t, 15000 A_t, and 18000 A_t were combined, respectively. A series of experiments were done varying influential parameters in order to obtain the full set of data for statistical analyses. For mechanical characterization, the Zwick/Roell Z 100 device was used. The mechanical properties S_0, R_m, R_p and A were obtained by tensile testing of samples, at room temperature according to Standard EN 10002-1.

2.1 Statistical analyses

Descriptive statistical analyses for all the obtained results have been expressed by means ± standard deviation (SD), in three repetitions, for each case of parameters. Collected data have been subjected to analysis of variance (ANOVA) for the comparison of means, and significant differences are calculated according to post-hoc Tukey's HSD ("honestly significant differences") test at $p < 0.05$ significant level, 95% confidence limit. The SOP models,[15,16] were obtained for independent variables (V, I and T), and the factors were rejected when their significance level was $p > 0.05$. The SOP models estimated the main effect of the process variables on the mechanical properties (S_0, R_m, R_p and A) during the EMC process of 7075 Al alloy. All SOP models were fitted to data collected by experimental measurements.

The experimental database is randomly divided into three groups for ANN model developing: training data (60%), cross-validation (used to test the performance of the network while training) (20%) and testing data (used to examine the network generalization capability) (20%). A multi-layer perceptron model (MLP) consisted of three layers (input, hidden and output), which is the most common, flexible and general-purpose kind of ANN was used,[17] giving the reason for choosing it in this study. The MLP neural network learns using an algorithm called "backpropagation". Levenberg–Marquardt algorithm is proved to be the fastest and particularly adapted for networks of moderate size. During this iterative process, input data are repeatedly presented to the network.[18] Furthermore, principal component analysis (PCA) has been applied successfully to classify and discriminate the different case of parameters. Pattern recognition technique has been applied within results descriptors to characterize and differentiate all varieties of observed cases.[19] Each of the statistical analyses has been performed using StatSoft Statistica 10.0® software.

2.2 Fuzzy synthetic optimization

Optimization procedure was performed using Fuzzy Synthetic Evaluation (FSE) algorithm,[20] implemented in Microsoft Excel 2007. FSE was implemented, using the results of models proposed to represent S_0, R_m, R_p and A, using eq. (1).

Trapezoidal membership function used in this calculation, could be written as,:[20]

$$A(x,a,m,n,b) = \begin{cases} a \le x < m, & \dfrac{x-a}{m-a} \\ m \le x < n, & 1 \\ n \le x < b, & 1 - \dfrac{x-n}{b-n} \end{cases} \quad (1)$$

where x is whether S_0, R_m, R_p and A, and the values of a, b, m and n are function parameters. Interval a–b represent the range in which measured values occurred, while range m–n is the expected optimal values range for output variables.

3. Results and Discussion

It is known the correlation between the microstructure and mechanical properties of an alloy.[21,22] When the microstructure is more uniform, consequently the mechanical properties are better. Our previous research shows[23,24] that electromagnetic casting has advantages over the conventional casting because the solidification process is changed.

The microstructure of samples was examined by optical microscopy using the image analysis device Leica Q500MC, after the usual metallographic preparation and etching in Keller's reagent (revealing morphology of Al segregation-solid solution and inter-metallic phase). The all samples were taken from the ingot center. The Fig. 2 presented the microstructure of samples obtained with different values of electromagnetic field frequency. The difference is obvious especially between the samples obtained with electromagnetic casting and without it.

Figure 2(a) reveals the typical microstructure of the conventionally cast EN AW 7075 Al alloy, while Fig. 2(b), 2(c) and 2(d) the microstructure of this alloy cast with influence of the electromagnetic field (with 10 Hz, 30 Hz and 50 Hz respectively). The samples obtained with electromagnetic casting process have more cellular and finer microstructure (especially with a frequency of 30 Hz) compared with dendritic microstructure in the sample obtained by conventional casting process.

This definitely affects the mechanical properties. Therefore, our further investigations were directed only to the electromagnetic casting process and the effect of operating parameters on the obtained mechanical properties values.

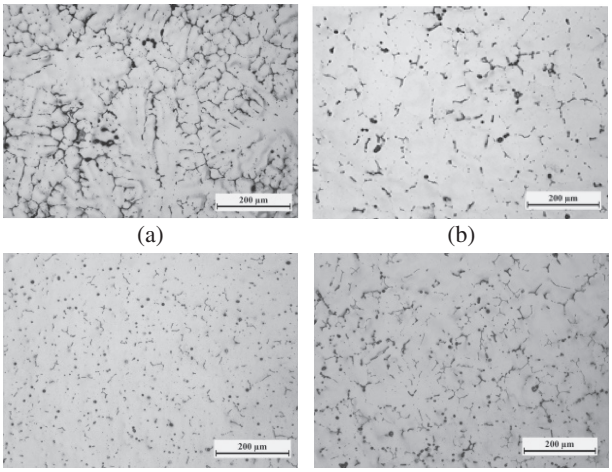

Fig. 2 Microstructure of sample cross section (a-0 Hz), (b-10 Hz), (c-30 Hz), (d-50 Hz), Keller's reagent, 100×.

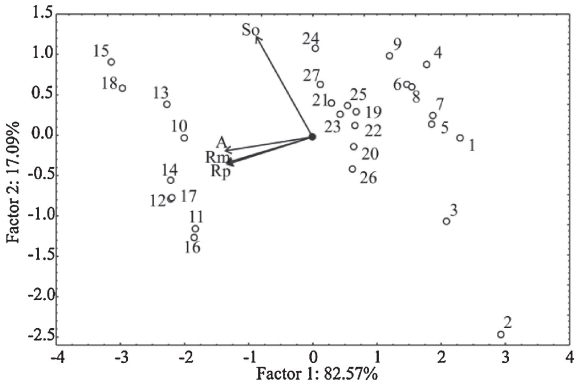

Fig. 3 Biplot of mechanical properties (S_0, R_m, R_p and A) for EN AW 7075 aluminum alloy.

Experimental data obtained were presented using basic descriptive statistics of obtained data, and post-hoc Tukey's HSD test, to represent significant differences between samples. Variables S_0, R_m, R_p and A varied significantly, imply that fitting of the experimental data could be performed using SOP or ANN modeling. Calculation of objective function F has been performed using eq. (1) accounting for 99.66% of the total variability can be considered sufficient for data representation and the first two principal components for used assays. R_m, R_p and A was found most influential for first factor coordinate calculation, while the S_0 was the most important variables for second factor coordinate calculation. The influence of V can be observed on Fig. 3, in which the samples with medium V values (30 Hz) are placed on the left side of graphic, while other samples (processed at 10 and 50 Hz) are located at the right side of graphic. Samples having the lowest factor 1 coordinate have had the highest R_m, R_p and A, and also the highest F values (samples No 15 and 18, and also 10, 12, 13 and 14). Samples located on the right side of PCA graph (No 1, 2 and 3) gained lower R_m, R_p and A values, and also the lowest F values.

3.1 Analysis of variance and SOP models

Analysis of variance (ANOVA) was conducted for obtained SOP models, and outputs were tested against the impact of input variables. According to ANOVA, responses S_0, R_m, R_p and A are mostly affected by V, statistically significant at $p < 0.05$. T variable was found also very influential, statistically significant at $p < 0.05$ and $p < 0.10$ levels, for these responses, while the impact of I was also noticed, but far less important. All response variables were mostly affected by quadratic terms of V, statistically significant at $p < 0.05$ level. Linear terms of V were also found statistically significant at $p < 0.05$ level.

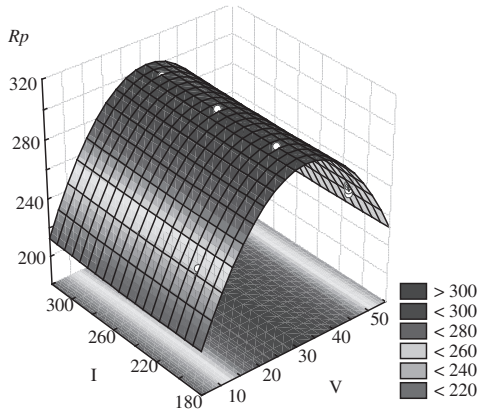

Fig. 4 R_p values under different I and V.

The residual variance, presents the model disagreement with the experimental values (contributions of other members that are not described in the SOP model). All developed models showed statistically insignificant deviation from the experimental values of the model, which confirmed their suitability. High r^2 values also indicated that the experimental data satisfactorily coincide with the mathematical models. A three-dimensional response surface plot was plotted for experiment data visualization and for the purpose of observation the fitting of SOP regression models to experimental data (Fig. 4).

3.2 ANN model

Broyden–Fletcher–Goldfarb–Shanno (BFGS) algorithm, implemented in StatSoft Statistica's evaluation routine, was used for ANN modeling. The optimization procedures to minimize the error function between network and experimental outputs was used during ANN training cycle,[25] and the sum of squares (*SOS*) was evaluated according to the BFGS algorithm, to speed up and stabilize convergence of the results.[26]

The training process was repeated several times in order to get the best performance of the ANN, due to a high degree of variability of parameters. It was accepted that the successful training was achieved when learning and cross-validation curves (*SOS* vs. training cycles) approached zero. Coefficient of determination (r^2) and *SOS* were used as parameters to check the performance (i.e. the accuracy) of the obtained ANN.

The optimum number of hidden neurons was chosen upon minimizing the difference between predicted ANN values and desired outputs, using *SOS* during testing as performance indicator. Used MLP is marked according to StatSoft Statistica's notation, "MLP" followed by number of inputs,

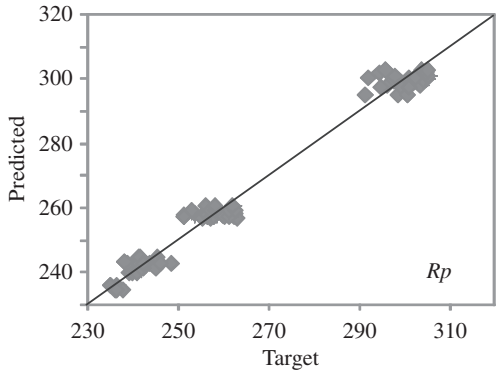

Fig. 5 Experimental measured and ANN model predicted values of R_p.

number of neurons in the hidden layer, and the number of outputs. According to ANN performance (sum of r^2 and SOSs for all variables in one ANN), it was noticed that the optimal number of neurons in the hidden layer is 8 (network MLP 3-8-4, with observed training performance 0.939 and training error 0.012).

The goodness of fit, between experimental measurements and model calculated outputs, represented as ANN performance (sum of r^2 between measured and calculated S_0, R_m, R_p and A), during training step were: 0.800; 0.970; 0.992 and 0.992, respectively.

ANN models were used to predict experimental variables (S_0, R_m, R_p and A). The networks were able to predict reasonably well all process outputs for a broad range of the process variables (as seen from Fig. 5, where the experimental measured and ANN model predicted values of R_p is presented).

The predicted values were very close to the desired values in most cases, in terms of r^2 value, for both SOP and ANN models. *SOS* obtained with ANN models are of the same order of magnitude as experimental errors for S_0, R_m, R_p and A reported in the literature.[26)]

It can be seen that these r^2 values for SOP models are very much alike to those associated with the ANN model. This agrees with other authors.[26)] Although ANN model are more complex (36–76 weights-biases for S_0, R_m, R_p and A) than SOP models, ANN models performed a bit better because of the high nonlinearity of the developed system.[27)] The values r^2 between experimental and SOP model outputs, for S_0, R_m, R_p and A, were: 0.531; 0.938; 0.986 and 0.977, respectively, while the best ANN model (MLP 3-8-4, No 3) gained: 0.800; 0.970; 0.992 and 0.992, respectively, during the training period.

3.3 Fuzzy synthetic optimization

Fuzzy synthetic optimization of the output variables was accomplished in order to find the V, I, T that give optimums of S_0, R_m, R_p and A. Trapezoidal membership function was used, according to eq. (1), in which a–b covered the complete interval of obtained output values, and m–n represented the optimal values (Table 1). The optimal parameters, used for FSE evaluation, were given based on our experience, calculating m as close, as possible to b.

The objective function (F), eq. (2), is the mathematical function whose maximum would be determined, by summing the FSE results, according to eq. (2). Each input parameter (V, I, T) has the equal influence on the function F:

$$F(V, I, T) = \overline{S_0} + \overline{R_m} + \overline{R_p} + \bar{A} \quad (2)$$

The maximum of function F represents the optimal V, I, T, and also the optimum of S_0, R_m, R_p and A. The values of F were determined using eq. (1). Values of membership function closer to 1 show the tendency of processing parameters to be optimal. Optimized process parameters (inputs and outputs) for all groups were shown in Table 2.

Table 1 Trapezoidal membership function parameters.

Parameter	S_0 mm^2	R_m N mm^{-2}	R_p N mm^{-2}	A %
a	49.88	321.56	235.72	3.01
b	50.49	405.75	302.53	6.86
m	50.46	385.46	287.40	6.51
n	50.49	405.75	302.53	6.86

Table 2 Optimizing parameters.

Optimal inputs		
V Hz	I A	T ($\times 10^{-3}$) At
30	250	18

Optimal outputs			
S_0 mm^2	R_m N mm^{-2}	R_p N mm^{-2}	A %
50.49	405.75	302.49	6.86

4. Conclusion

The electromagnetic casting process has more advantages than the conventional casting, but the efficiency of the process depends on operating parameters. It is known that by combining the operating parameters it is possible to obtain good quality of as cast ingots. This is very important because of lowering energy consumption and saving time. There is only one question: "Which combination of operating parameters is the best?" Through the SOP and ANN based mathematical models it is possible to obtain the answer, so this work presents the further step and a new approach in improving the electromagnetic casting process. SOP and ANN based models were developed for prediction of S_0, R_m, R_p and A for a wide range of experimental conditions. Models were able to predict successfully experimental data, with ease of implementing it for design and control of the processes and also the effective use for predictive modeling and optimization. SOP models yield quite good fit of experimental data, according to r^2. As compared to SOP models, ANN models yield a bit better fit of experimental data, according to r^2 and SOS of both models. Taking into account that a considerable amount and wide variety of data were used in the present work to obtain the SOP models, and considering that the model turned out to yield a sufficiently good representation of these data, these models can be expected to be very useful in practice for the design and control the EMC process of 7075 Al alloy.

Acknowledgement

The authors are grateful to the Ministry of Education, Science and Technological Development of the Republic of Serbia for the financial support of this investigation included in the projects TR 34002 and TR 31055.

REFERENCES

1) Z. Zhao, B. Zuo and J. Wang: Acta Metall. Sin. **43** (2007) 956–960.
2) Z. Zhao, C. Jianzhong and D. Jie: J. Mater. Process. Technol. **182** (2007) 185–190.
3) H. Yongdong, Z. Xinming and C. Zhiqiang: Chin. Foun. J. **6** (2009) 214–218.
4) J. A. Wagner and R. N. Shrenoy: Metall. Mater. Trans. A **22** (1991) 2809–2818.
5) Z. Beijiang, L. Guimin and C. Jianzhong: J. Mater. Sci. Technol. **18** (2002) 401–403.
6) B. Zhang, J. Cui, G. Lu, Q. Zhang and C. Ban: Trans. Nonferrous. Met. Soc. China. **13** (2003) 158–161.
7) J. Dong, C. Jianzhong, Y. Fuxiao, B. Chunyan and Z. Zhihao: Metall. Mater. Trans. **35** (2004) 2487–2494.
8) Y. Zuo, C. Jianzhong, D. Jie and Y. Fuxiao: J. Alloy. Compd. **402** (2005) 149–155.
9) J. Dong, J. Cui, F. Yu, Z. Zhao and Y. Zhuo: J. Mater. Process. Technol. **171** (2006) 399–404.
10) J. Cui, Z. Zhang and Q. Le: Trans. Nonferrous. Met. Soc. China **20** (2010) 2046–2050.
11) Z. Yubo, J. Cui, Z. Zhao, H. Zhang and K. Qin: Mater. Sci. Eng. A **406** (2005) 286–292.
12) J. Zhang, Z. Cui and M. Lu: Acta Metall. Sin. **38** (2002) 215–218.
13) Y. Jin and C. Li: Acta Metall. Sin. **27** (1991) 317–323.
14) G. Annadurai, L. Lai and L. Jiunn: Afr. J. Biotech. **6** (2007) 296–303.
15) Anonymous (2012) Engineering Statistics Handbook, http://www.itl.nist.gov/div898/handbook/pri/section1/pri11.htm. Accessed in September 2013.
16) Anonymous (2012) Engineering Statistics Handbook, http://www.itl.nist.gov/div898/handbook/pri/section3/pri333.htm. Accessed in September 2013.
17) M. Arsenović, Z. Radojević, S. Stanković, Ž. Lalić and L. Pezo: Ceram. Int. **39** (2013) 1667–1675.
18) S. Grieu, O. Faugeroux, A. Traoré, B. Claudet and L. Bodnar: Energy Build. **43** (2011) 543–554.
19) M. Otto: *Chemometrics: Statistics and Computer Application in Analytical Chemistry*, (Wiley-VCH, Weinheim, Germany, 1999) pp. 95–123.
20) T. Brlek, L. Pezo, N. Voća, T. Krička, Đ. Vukmirović, R. Čolović and M. Bodroža: Fuel. Process. Technol. **116** (2013) 250–256.
21) G. Wang, H. Zhao, Z. Cui and Q. Guo: Acta Metall. Sin. Engl. Lett. **2** (2012) 160–168.
22) W. Shuang, Z. Yubo and C. Jianzhong: Chin. Foun. J. **4** (2007) 280–283.
23) A. Patarić, Z. Gulišija and S. Marković: Prakt. Metallogr. **44** (2007) 290–298.
24) A. Patarić, M. Mihailović and Z. Gulišija: J. Mater. Sci. **47** (2012) 793–796.
25) J. Taylor: *Methods and Procedures for the Verification and Validation of Artificial Neural Networks*, (Springer Science and Business Media, Inc., USA, 2006) pp. 73–98.
26) A. Basheer and M. Hajmeer: J. Microbiol. Meth. **43** (2000) 3–31.
27) L. Pezo, Lj. Ćurčić, S. Filipović, R. Nićetin, B. Koprivica, M. Mišljenović and B. Lević: Hem. Ind. (2013) DOI:10.2298/HEMIND120529082P.